GLOWORM-PARA: a flexible framework to simulate the population dynamics of the parasitic phase of gastrointestinal nematodes infecting grazing livestock

Journal Pre-proofs

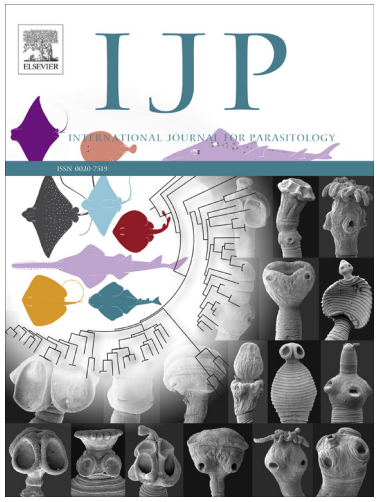

GLOWORM-PARA: a flexible framework to simulate the population dynamics of the parasitic phase of gastrointestinal nematodes infecting grazing livestock

H. Rose Vineer, S.H Verschave, E. Claerebout, J. Vercruysse, D.J. Shaw, J. Charlier, E.R. Morgan

PII: S0020-7519(20)30005-9
DOI: https://doi.org/10.1016/j.ijpara.2019.11.005
Reference: PARA 4228

To appear in: *International Journal for Parasitology*

Received Date: 27 May 2019
Revised Date: 22 November 2019
Accepted Date: 29 November 2019

Please cite this article as: Rose Vineer, H., Verschave, S.H, Claerebout, E., Vercruysse, J., Shaw, D.J., Charlier, J., Morgan, E.R., GLOWORM-PARA: a flexible framework to simulate the population dynamics of the parasitic phase of gastrointestinal nematodes infecting grazing livestock, *International Journal for Parasitology* (2020), doi: https://doi.org/10.1016/j.ijpara.2019.11.005

GLOWORM-PARA: a flexible framework to simulate the population dynamics of the parasitic phase of gastrointestinal nematodes infecting grazing livestock

Rose Vineer, H.[a,b,c,*], Verschave, S. H.[d,e], Claerebout, E.[d], Vercruysse, J.[d], Shaw, D.J.[f], Charlier, J.[g], Morgan, E. R. [a,b,h]

[a] *Veterinary Parasitology and Ecology Group, Bristol Veterinary School, University of Bristol, UK, BS8 1TQ*

[b]*Cabot Institute, Royal Fort House, University of Bristol, UK, BS8 1UJ*

[c] *Department of Infection Biology, Institute of Infection and Global Health, University of Liverpool, Leahurst Campus, Neston, Cheshire, UK, CH64 7TE*

[d]*Department of Virology, Parasitology and Immunology, Faculty of Veterinary Medicine, Ghent University, Salisburylaan 133, 9820 Merelbeke, Belgium*

[e]*Department of Molecular and Cellular Biology, Harvard University, 52 Oxford Street, Cambridge, MA 02138, USA*

[f]*The Royal (Dick) School of Veterinary Studies and The Roslin Institute, University of Edinburgh, Easter Bush Campus, Roslin, EH25 9RG, United Kingdom*

[g]*Kreavet, Hendrik Mertensstraat 17, 9150 Kruibeke, Belgium*

[h]*Institute for Global Food Security, Queen's University Belfast, UK, BT9 7BL*

*Corresponding author. *E-mail address*: hannah.vineer@liverpool.ac.uk

ABSTRACT

Gastrointestinal (GI) nematodes are a significant threat to the economic and environmental sustainability of keeping livestock, as adequate control becomes increasingly difficult due to the development of anthelmintic resistance (AR) in some systems and climate-driven changes to infection dynamics. To mitigate any negative impacts of climate on GI nematode epidemiology and slow AR development, there is a need to develop effective, targeted control strategies that minimise the unnecessary use of anthelmintic drugs and incorporate alternative strategies such as vaccination and evasive grazing. However, the impacts climate and GI nematode epidemiology may have on the optimal control strategy are generally not considered, due to lack of available evidence to drive recommendations. Parasite transmission models can support control strategy evaluation to target field trials, thus reducing the resources and lead-time required to develop evidence-based control recommendations incorporating climate stochasticity. GI nematode population dynamics arising from natural infections have been difficult to replicate and model applications have often focussed on the free-living stages. A flexible framework is presented for the parasitic phase of GI nematodes, GLOWORM-PARA, which complements an existing model of the free-living stages, GLOWORM-FL. Longitudinal parasitological data for two species that are of major economic importance in cattle, *Ostertagia ostertagi* and *Cooperia oncophora,* were obtained from seven cattle farms in Belgium for model validation. The framework replicated the observed seasonal dynamics of infection in cattle on these farms and overall, there was no evidence of systematic under- or over-prediction of faecal egg counts (FECs). However, the model under-predicted the FECs observed on one farm with

48 very young calves, highlighting potential areas of uncertainty that may need further
49 investigation if the model is to be applied to young livestock. The model could be
50 used to drive further research into alternative parasite control strategies such as
51 vaccine development and novel treatment approaches, and to understand GI
52 nematode epidemiology under changing climate and host management.
53
54 *Keywords*: *Ostertagia ostertagi*; *Cooperia oncophora*; Model; Parasite; Population
55 dynamics; Transmission; Nematode; Livestock
56

1. Introduction

Gastrointestinal (GI) nematodes are increasingly recognised as an important threat to the future sustainability of keeping livestock for food production and leisure. At a policy level, livestock make a significant contribution to agricultural greenhouse gas (GHG) emissions, which may be exacerbated by GI nematode infections (Fox et al., 2018). In 2013, methane emissions from cattle and sheep were responsible for 47% of agricultural GHG emissions in England, and approaching 90% of agricultural GHG emissions in Wales, Scotland and Northern Ireland (Salisbury et al., 2015). GI nematodes also threaten food security and the economic sustainability of livestock farming as they cause significant production losses in ruminants (Nieuwhof and Bishop, 2005; Charlier et al., 2009). For example, a meta-analysis of 88 studies found that lambs infected with GI nematodes experienced a 25% reduction in weight gain (Mavrot et al., 2015). Similarly, in cattle, GI nematodes cause significant reductions in weight gain and milk yield (Verschave et al., 2014b). Finally, the pathogenic implications of GI nematode infections (e.g. Besier et al., 2016) on host welfare are clear, however the impact of subclinical and chronic infections remains an understudied but important question in livestock helminth research (Morgan et al., 2018).

Currently, the control of GI nematodes in livestock is primarily based on the chemotherapeutic use of anthelmintic substances (Charlier et al., 2014). However, both the influence of climate change and, in some places, the development of AR on farm management and parasite epidemiology are expected to challenge the future control of these infections (Morgan and van Dijk, 2012; Skuce et al., 2013). Progress has been made towards targeted, sustainable control strategies that are

economically sound (Charlier et al., 2014) but the need for adequate decision-support tools to aid in the implementation of these strategies remains (Morgan, 2013). Multiple initiatives promoting the sustainable control of parasites in livestock have been developed worldwide, such as SCOPS (Sustainable Control of Parasites in Sheep; scops.org.uk), COWS (Control of Worms Sustainably; cattleparasites.org.uk), the UK-VET guidelines on parasite control in horses (Rendle et al., 2019) in the UK, and ASKBILL (Kahn et al., 2017) in Australia. These initiatives provide flexibility to adapt their guidelines to different livestock management systems and, in the case of SCOPS, resource-intensive longitudinal studies evaluating the efficacy of their guidelines in a range of systems are ongoing (e.g. Learmount et al., 2018).

However, the epidemiology of GI nematode infections is a result of complex interactions between parasite, host, climate, farm management and historic control strategies. The efficacy of these guidelines in the diversity of management systems practiced by cattle, sheep, goat and horse keepers worldwide, and their sustainability in the face of climate change and AR cannot be studied empirically without significant resource input and multi-year studies to incorporate inter-annual weather variability and extreme weather events.

Parasite transmission models are useful as they provide the potential to include a variety of processes on different levels and extrapolate current knowledge to alternative scenarios at large temporal scales (Rose et al., 2015). In doing so, model simulations can be used to target resources for empirical research where they are needed most, and guide the development of evidence-based parasite control strategies and tools. The development of mathematical models to simulate the transmission dynamics of GI nematode infections in ruminants dates back several

decades. The majority of the existing models were developed specifically for GI nematode infections in sheep (Verschave et al., 2016a lists 32 models). Fewer models exist for cattle nematodes (Verschave et al., 2016a lists seven models for *Ostertagia ostertagi*), and model development for equine nematode species dates back only a few years (Leathwick et al., 2015, 2016, 2017). Generic models that provide a framework for GI nematode infections that can be applied to a range of host and nematode species are also scarce (Smith, 2011), while their development is of great interest in identifying emerging patterns of change (Molnár et al., 2013; Rose et al., 2014).

Recently, a generic model framework for the free-living phase of GI nematodes, which has important modifications on behaviour and development of the larvae on pasture, was developed (GLOWORM-FL, Rose et al., 2015). This model was initially applied to three species of importance in cattle (*O. ostertagi*) and small ruminants (*Haemonchus contortus* and *Teladorsagia circumcincta*), and additional published parameters and data are available to adapt the model to equine cyathostomins (Leathwick et al., 2015), *Cooperia oncophora* in cattle (Sauermann and Leathwick, 2018) and *Marshallagia marshalli* in small ruminants (Carlsson et al., 2013). To fully explore the consequences of different control and management approaches on parasite epidemiology, however, a complementary model for the parasitic phase is needed as host-parasite interactions and host acquired immunity play crucial parts in the transmission dynamics of GI nematodes (Claerebout and Vercruysse, 2000).

The aim of the current study was to develop a conceptual model framework for the parasitic phase of GI nematodes, GLOWORM-PARA, that can be applied to a range of host and parasite species. Here, the model is parameterised and validated

for two species that are of major economic importance in cattle, i.e. *O. ostertagi* and *C. oncophora.* Previous cattle models have tended to only focus on one nematode species, i.e. *O. ostertagi*, perhaps due to its pathogenic significance compared with *C. oncophora*, against which cattle develop an effective immune response. No single-species model exists for *C. oncophora,* despite its increasing importance in the context of anthelmintic resistance and treatment failure (Sutherland and Leathwick, 2011). The development of acquired immunity against GI nematodes was modelled and parameterised in a heuristic but data-driven manner, to provide a transparent and replicable approach. An extensive set of field observations of first season grazing cattle was used for model validation.

2. Materials and methods

2.1. Model framework

The model framework (Fig. 1), tracks the mean number of GI nematodes and level of acquired immunity in a group of hosts (i.e. is a population-based mean-field model). State variables and model parameters are defined in Table 1.

Infective L3 are ingested with herbage (*L3i*) and enter the pool of pre-adult parasitic nematodes (*P*). Pre-adult nematodes either develop to adult nematodes (*A*) or arrest their development as larvae (*Pa*) before developing to the adult stage. Although the model is developed and validated for trichostrongylid nematodes in the present study, it could also be applied to other strongylid species with a broadly similar life cycle (e.g. equine cyathostomins) as all pre-adult stages are modelled as a single state variable and the pre-adult stage involved in arrested development is not specified. This basic representation of the GI nematode life cycle is similar to

numerous previous models, as reviewed by Verschave et al. (2016a) and Smith (2011).

$$\frac{dP}{dt} = L3i - \delta P - \mu_1 P \quad (1)$$

$$\frac{dPa}{dt} = -h_2\mu_2 Pa + \delta h_1 P \quad (2)$$

$$\frac{dA}{dt} = \delta(1 - h_1)P + h_2 Pa - \mu_3 A \quad (3)$$

Acquired immunity (*r*) increases in response to exposure to infection (Claerebout and Vercruysse, 2000), in this case the L3 ingestion rate (*L3i*), and decays with time, similar to previous models e.g. Roberts and Grenfell (1991). However, the present framework differs from previous models in its representation of *r* as a logistic growth function to facilitate modelling interactions between the host immune response and parasite life-history parameters (Section 2.3.3).

$$\frac{dr}{dt} = \rho(L3i)(1 - r) - \sigma r \quad (4)$$

2.2. Model integration

The model was implemented in R v 3.5.1 "Feather Spray" (R Core Team, 2018. R: A language and environment for statistical computing. R Foundation for Statistical Computing, Vienna, Austria) using the *lsoda* function of the *deSolve* package v 1.24 (Soetaert et al., 2010) for solving differential equations. The model returns daily output. Anthelmintic treatments (if applicable) are implemented using the *events* argument of the *lsoda* function to reduce the worm burden by a representative percentage for the duration of the residual activity of the product used. For example,

an effective moxidectin pour-on treatment for cattle would trigger a reduction in total worm burden of 99% for 35 days. The percentage of reduction could be modified, if necessary, to represent vaccination strategies or reduced anthelmintic efficacies observed in the field. Model output is the mean stage-specific worm burden and egg output per host, which can be used to estimate the faecal egg count (FEC; eggs per gram of faeces (epg)) if the amount of faeces produced is known.

2.3. Parameter estimates

Parameterisation of the framework for multiple species is demonstrated using two species infecting cattle that are currently the focus of vaccine development programmes (Matthews et al., 2016): the abomasal nematode *O. ostertagi* and the intestinal nematode *C. oncophora* (Table 2).

2.3.1. Seasonally variable parameters

Arrested development. There is currently no consensus on the mechanisms of arrested (hypobiosis) and subsequent resumed development in trichostrongylid nematodes, and numerous confounding factors in available data prevent the development of robust mechanistic models of arrest (Smith, 1974; Michel et al., 1976; Frank et al., 1986; 1988; Eysker, 1993; Fernández et al., 1999; Langrova and Jankovska, 2004; Lützelschwab et al., 2005; Langrova et al., 2008). As the numerous potential drivers of arrest are correlated and seasonal (e.g. the age structure of host populations, host immunity, temperature, moisture and photoperiod), a simplified seasonal approach was taken to estimate seasonal variations in the factor driving

arrest rates *(d)* which is used to simulate the proportion of developing pre-adult nematodes that enter a state of arrested development (h_1).

For *C. oncophora* and *O. ostertagi* this arrest rate (h_1) was assumed to be related to the development success of eggs and larvae on pasture. *d* was approximated as a 7 day moving average, determined by the temperature-dependent development rate (using the *na.ma* function in the *imputeTS* R package v 3.0 (Moritz and Bartz-Beielstein, 2017) and the *ma* function in the *forecast* package v 8.9 (Hyndman and Khandakar, 2008)), whereby the minimum arrest rate is assumed to coincide with the period where development success is at its maximum and the maximum arrest rate is assumed to coincide with the period where development success is at its minimum. Thus, the arrest rate at the current time point, *t,* is a function of the species-specific minimum and maximum arrest rates (h_{min} *and* h_{max}), annual minimum and maximum predicted development success at the study site (d_{min} *and* d_{max}), and predicted development success at the current timestep (d_t).

$$h_1 = h_{(max)} - \left(\frac{h_{(max)} - h_{(min)}}{d_{(max)}}\right) \times d_t \quad (5)$$

The temperature-dependent development rate of eggs and larvae on pasture for *O. ostertagi* was as described in Rose et al. (2015). For *C. oncophora,* development rate data presented in Sauermann and Leathwick (2018) were extracted using Plot Digitizer v2.6.8 (http://plotdigitizer.sourceforge.net/), and a linear model applied to the data using the *lm()* function in R.

214 The proportion of arrested larvae resuming development (h_2) was assumed to be
215 an inverse function of the driver of arrest (i.e. development success for *O. ostertagi*
216 and *C. oncophora)*:
217

$$h_2 = \left(\frac{1}{d_{(max)} - d_{(min)}}\right) \times (d_t - d_{(min)}) \quad (6)$$

218

219 *L3 ingestion rate and dry matter intake.* To calculate the L3 ingestion rate (*L3i*) the
220 average daily dry matter intake (DMI) by grazing cattle was estimated using the
221 equations of MAFF (1975) based on bodyweight (estimated from the bodyweight at
222 turn out using standard age-related growth curves for dairy cattle; Cue et al., 2012,
223 Verschave et al., 2014a). The equations for growing young stock and adult cattle
224 were used for animals with a bodyweight of less than and more than 400 kg,
225 respectively. The rate of ingestion of dry matter was estimated as a proportion of
226 the total available herbage consumed (*kgDM*; standing biomass, i.e. kilograms of dry
227 matter per hectare). From this, the L3 ingestion rate was estimated as follows
228 (parameter and state variables are defined in Table 1):

$$L3i = -ln\left(1 - \frac{DMI}{kgDM}\right) \times L3h \quad (7)$$

229

230 *Faeces production and faecal egg counts.* The average daily faeces production
231 was estimated based on host body weight using the formula of Nennich et al. (2005).
232 Mean FECs (epg) for the group of hosts can be estimated from the number of adults
233 (A), per adult fecundity rate (λ) and expected daily faeces production (f).

$$\mathrm{FEC} = \frac{\mathrm{A}e^{\lambda}}{\mathrm{f}} \quad (8)$$

234

235 *2.3.2. Constant rates*

236 The development rate (δ) from ingested L3 to mature adult was estimated from a
237 prepatent period of 17 days for both *O. ostertagi* and *C. oncophora;* (Table 2; Powers
238 et al., 1982).

239 No data were available in the literature to estimate the mortality rates of arrested
240 larvae due to the confounding effects of resumed development. Therefore, the
241 mortality rate of arrested L4s for both *O. ostertagi* and *C. oncophora* was set at 0.002
242 after Grenfell et al. (1987). Mortality rates of all other pre-adult and adult
243 nematodes were a function of immunity (section 2.3.3).

244

245 *2.3.3. Immunity and dependent parameters*

246 *Immune response and decay rate.* No data were available to formally estimate
247 immunity decay rates (σ) for *O. ostertagi* nor *C. oncophora*, therefore three experts
248 in the area of cattle GI nematodes and vaccine development (J. Vercruysse, E.
249 Claerebout (both co-authors on this study) and P. Dorny, Ghent University, Belgium)
250 were consulted in order to estimate the percentage of decay in immunity over a
251 typical housing period.

252 To estimate the response rate (*ρ*), it was assumed that protective immunity (*r*=1)
253 was typically acquired after 1.5 grazing seasons (9 months of exposure punctuated
254 by a 6 month housing period during which immunity is assumed to decay as
255 described above) for *O. ostertagi* and one grazing season (6 months) for *C.*

256 *oncophora* (Armour, 1989; Ploeger et al., 1995; Claerebout et al., 1998; Ravinet et
257 al., 2014). Species-specific field observations of L3 density on pasture (*L3h*) over the
258 course of a grazing season were extracted from the raw data from field trials across
259 Europe summarised by Shaw et al. (1998). The data concerned pasture larval counts
260 from both 'clinical' and 'subclinical' pastures (i.e. pastures on which an outbreak of
261 parasitic gastroenteritis in the untreated first season grazers was observed, or not,
262 respectively) and included a mixture of calves that were treated with anthelmintics
263 and untreated controls (Shaw et al., 1998). Using these data, equation 4, the decay
264 rate (σ) and the method described in section 2.3.1 for estimating L3 intake rates, the
265 *optimise* function in R was used to find the response rate that minimised the sum of
266 square error (SSE) for each dataset, given the expectation that *r* should equal 0.4 and
267 0.6 after 3 months of grazing, and 0.7 and 1 after 6 months of grazing for *O. ostertagi*
268 and *C. oncophora,* respectively.
269
270 *Immunity-mediated regulation of the parasite population.* Host acquired
271 immunity is assumed to regulate the parasite population in three ways: (i) by
272 exclusion of ingested larvae (increased pre-adult mortality rate); (ii) by decreasing
273 the survival of established (adult) nematodes; and (iii) by decreasing the fecundity of
274 adult nematodes (Barger et al., 1985; Smith and Grenfell, 1985; Coyne and Smith,
275 1992; Smith, 1994; Stear et al., 1995; Claerebout and Vercruysse, 2000; Garnier et
276 al., 2016). Thus immunity-mediated regulation of the parasite population was
277 incorporated by increasing the mortality rates of pre-adult (μ_1) and adult nematodes
278 (μ_3), and decreasing fecundity (λ) with increasing acquired immunity. As acquired
279 immunity cannot be measured directly (Claerebout and Vercruysse, 2000), little is

known about the functional relationship between acquired immunity and these parameters. Therefore, a linear relationship was assumed, whereby mortality increases between the minimum and maximum values, and fecundity decreases between the maximum and minimum values as acquired immunity increases between 0 and 1:

$$\mu_i = \mu_{i(min)} + (\mu_{i(max)} - \mu_{i(min)})r \quad (9)$$

$$\lambda = \lambda_{(max)} - (\lambda_{(max)} - \lambda_{(min)})r \quad (10)$$

2.4. Model validation

2.4.1. Longitudinal data

The model was validated using independent datasets containing longitudinal parasitological data collected during 2012 and 2013 (described in detail in Verschave, S.H., 2015. Development of a transmission model for gastro-intestinal nematode infections in cattle. PhD thesis. Ghent University, Belgium) and summarised in Supplementary Table S1. The sampled herds consisted of first season grazers located on seven commercial dairy farms in Flanders (Belgium). The herds were visited monthly from turn out in Spring (April, May or June) until housing in Autumn (September, October or November).

FECs of all animals were performed each month using a modified McMaster technique with a sensitivity of 10 epg (MAFF, 1986) and the mean and 95% confidence interval estimated for each month. For this, the *sample* and *replicate*

functions in R were used to generate 10,000 replicates sampling with replacement. The *quantiles* function was then used with probabilities of 0.025 and 0.975 to obtain the bootstrapped 95% confidence limits for the means of these replicates.

For nematode species identification, the positive faecal samples were mixed per herd, cultured and identified according to Borgsteede and Hendriks (1973). Pasture infectivity (density of L3 on herbage; *L3h*) was measured as described in Verschave et al. (2015) each month and every 2 months, respectively, in 2012 and 2013 using the modified technique of Taylor (1939).

2.4.2. Validation simulations

Mean FECs and 95% confidence intervals reported by Verschave (Verschave, S.H., 2015. PhD thesis, cited earlier) were corrected for incomplete egg recovery (recovery rate of 55%; Paras et al., 2018). Corresponding daily pasture contamination values for the entire period of each trial were obtained by interpolation of the monthly pasture contamination values using the *approxfun* function in R. The data collected from each herd formed a separate validation dataset.

Daily mean air temperature data used to estimate daily values for development success to estimate arrest rates (equations 5 and 6) were obtained for each herd from the E-OBS gridded dataset (Haylock et al., 2008; dataset available to download from https://www.ecad.eu/download/ensembles/download.php) based on the location of the village where each herd was located (Supplementary Table S1) using the *ncdf4* function v 1.17 in R (Pierce, D. 2019. ncdf4: Interface to Unidata netCDF (Version 4 or Earlier) Format Data Files. R package version 1.17. https://CRAN.R-project.org/package=ncdf4).

326 The longitudinal field observations were used to validate species-specific
327 deterministic model simulations. Daily L3 intake rates were estimated from the
328 interpolated field data as described in equation 7. Dry matter intake and faeces
329 production were estimated as described in section 2.3.1. No data were available for
330 standing biomass, therefore, 2000 kg of DM per hectare was assumed. Although the
331 individuals in the longitudinal datasets were first season grazers (i.e. had never had
332 exposure to *O. ostertagi* nor *C. oncophora*), there is potential for age-related
333 immunity due to the maturation of the immune system (see discussion in Vercruysse
334 and Claerebout, 1997, and Smith et al., 1985). Therefore, host immunity (*r*) was set
335 at an initial value between 0.1 and 0.5, dependent on age at the start of the grazing
336 period (i.e. 6 months of age, r = 0.1; 21 months of age, r = 0.5).
337
338 *2.4.3. Statistical validation: deterministic simulations*
339 Model goodness of fit was assessed using a linear regression through the origin of
340 observed and predicted FECs as described by Rose et al. (2015). The first FEC for
341 each herd was excluded from statistical validation as this FEC was simply to confirm
342 the absence of infection at turn out. A statistically significant regression with low
343 residual error indicates that the model reproduces the seasonal patterns of the
344 observed FECs. However, statistical significance does not validate the ability of the
345 model to reproduce the magnitude of FECs observed. For this, the slope estimate
346 was used. A perfect linear fit between model predictions and field observations
347 implies an intercept of zero and a slope of 1. A regression through the origin with a
348 slope that is not significantly different from 1, and therefore included in the 95%
349 confidence interval, indicates that the model reproduces the magnitude of observed

FECs over the course of the season, with values significantly less than 1 indicating underestimation of FECs and values significantly greater than 1 indicating overestimation of FECs. A high R^2 value indicates that the model captures a significant proportion of the variance in the observed FECs. Due to the relatively small number of individuals in each herd, the potential for considerable individual variation in FECs (Levecke et al., 2011), and the limitations of the McMaster's faecal egg counting method and other flotation techniques (Egwang and Slocombe, 1981), visual comparison of observed and predicted values were incorporated into the evaluation to mitigate against this variability undermining statistical validation.

2.4.4. Qualitative validation: stochastic simulations

Although the framework presented here is a deterministic mean-field model representing a group of hosts, incorporating individual variation is possible and is beneficial for further validation and future evaluation of individual-based parasite control strategies. An additional 50 simulations were run per herd, per nematode species (representing 50 individual hosts) to incorporate the stochastic influences of between-host variation. The aggregation of *L3h* and chance encounters with *L3h* during grazing was incorporated as described in Berk et al. (2016b). The L3 ingestion rate was drawn from a negative binomial distribution using the *rnbinom* function in R, with a mean equal to the observed *L3h* at each time point, and a high level of aggregation, as would be expected for the moderate *L3h* densities observed in this study (k = 1.41; Verschave et al., 2015). For other species or farming systems, the mean and aggregation values could be adapted to reflect the characteristics of the system to be modelled. In addition to stochastic L3 ingestion, between-host

variability in immune response was drawn from a negative binomial distribution with a mean equal to ρ and level of aggregation equal to that used for the L3 intake rate, after Stear et al. (2007) suggested that the distribution of the immune response between hosts mirrored that of the parasitological variables.

The practical significance of deviations in model predictions from the observed FECs was also considered in the context of the hypothetical use of the simulated FECs to guide further risk assessment (e.g. prompting a FEC or weighing) and potentially trigger anthelmintic treatment in cattle. Fifty to 200 epg is considered a "Medium" to "High" risk egg count (COWS, 2014). Therefore, a deviation of 200 epg in predicted FECs within the range of 0-400 epg could theoretically result in incorrect risk assessment and anthelmintic treatment choices.

3. Results

3.1. Parameter estimates

Linear regression of the development rates reported by Sauermann and Leathwick (2018) against temperature for *C. oncophora* yielded a statistically significant fit (a = -0.04, b = 0.008, R^2 = 0.8166, R^2adjusted = 0.8058, $F_{(1,17)}$ = 75.7, p = 1.142e-07) with a predicted minimum development threshold of 5°C (minimum threshold for development = (0-a)/b).

Expert opinion placed the estimated decay rate over an average 6 month housing period (Charlier et al., 2010) at between 10% and 50%. Therefore, a 6 month decay rate of 30% was used to estimate a daily decay rate (Table 2).

Using optimisation to fit the response rate (ρ) to data from Shaw et al. (1998) yielded a median response rate for *O. ostertagi* of 0.00006 (inter-quartile range (IQR)

0.00024) with a median SSE of 0.03205 (IQR 0.32502). For *C. oncophora* this yielded a median response rate of 0.00013 (IQR 0.00040) with a median SSE of 0.00250 (IQR 0.11904). The median fitted response rate was used in all subsequent simulations.

All other parameter estimates are provided in Table 2.

3.2. Model validation

The R code used for model simulations and validation is provided in Supplementary Data S1. The code can be viewed and run in R software, or viewed in a plain text editor.

Daily temperature and rainfall data are shown for the location of each herd in Supplementary Fig. S1. The average age at turn out varied between 6 and 21 months (Verschave, S.H., 2015. PhD Thesis, cited earlier; Supplementary Table S1). With the exception of herd 2, longitudinal FEC data used for model validation (Figs. 2 and 3; Supplementary Data S1) tended to be low throughout the grazing season. Mean pasture larval counts (L3h kg DM^{-1}) were low at turnout, ranging from 0.001 to 176 L3h kg DM^{-1} (Supplementary Table S1), potentially accounting for the low FECs. However the FECs used for validation are typical for calves in their first grazing season with subclinical infections (Shaw et al., 1997).

Qualitatively, species-specific simulations for *O. ostertagi* and *C. oncophora* reproduced general observed patterns of FECs over the course of a grazing season in first season grazers (Figs. 2 and 3). Overall, the model captured a high proportion of variance in the observed FECs for both *O. ostertagi* (mean R^2 = 0.76) and *C. oncophora* (mean R^2 = 0.67), and residual error was low (Table 3). A statistically

421 significant regression through the origin was achieved for 6/7 (*O. ostertagi*) and 3/7
422 (*C. oncophora*) of the validation datasets (Table 3; Fig. 4).

423 For *O. ostertagi,* there were both negative and positive deviations in the slope
424 from 1 (Table 3), indicating under- or over-prediction of FECs, respectively. However,
425 as the model both under- and over-predicted FECs, there was no evidence of
426 systematic bias. Significant deviations in the slope from 1 were estimated for three
427 of the herds (Table 3). Qualitative assessment of model fit against the mean model
428 and 50 individual simulations incorporating individual variation in immune response
429 and the aggregation of L3s on pasture (Fig. 2) suggests that these deviations are of
430 no practical significance (section 2.4.4), with the exception of Herd 2, where high
431 FECs were observed at the end of the grazing season while predicted FECs remained
432 low.

433 For *C. oncophora*, there were predominantly negative deviations in the slope
434 from 1, indicating underprediction of FECs. A significant deviation in the slope from 1
435 was estimated for five of the herds (Table 3). Nevertheless, qualitative assessment as
436 above (Fig. 3) suggests that these deviations, similar to the *O. ostertagi* simulations,
437 are of little practical significance (section 2.4.4). Herd 2 was, again, an exception,
438 with higher FECs observed than predicted.

439

440 **4. Discussion**

441 Smith noted, in 2011, that "*Although it was eventually realised that within each*
442 *class of parasites a single generic model framework with suitably adjusted parameter*
443 *values could satisfactorily represent almost all the infections of interest… most of the*
444 *examples of nematode and trematode models in the literature were constructed on*

445 *an ad hoc basis to address issues dealing with control of a specific parasite in a*
446 *specific host in a specific country*". Although many of the models published in recent
447 decades contain important differences in the focus of detail necessary for the
448 specific application of the model (e.g. Cornell et al., 2004; Laurenson et al., 2011),
449 more widely applicable models use proprietary software (e.g. Learmount et al.,
450 2006) or are developed using complex spreadsheets (e.g. Sauermann and Leathwick
451 2018) that can be difficult to reproduce. Furthermore, differences in the structure of
452 the various model frameworks available and their parameters prevent direct
453 comparisons between model outputs.

454 Here, GLOWORM-PARA, a generic model framework for the parasitic phase of GI
455 nematode infections is presented. The model can be adapted to different host and
456 nematode species and was developed to complement a previously published model
457 of the free-living stages (GLOWORM-FL; Rose et al., 2015). The model's flexibility is
458 demonstrated by parameterisation for two economically important trichostrongylid
459 species infecting cattle worldwide, *C. oncophora* and *O. ostertagi,* and validation
460 against multiple independent datasets. To our knowledge, no previous attempt has
461 been made to model *C. oncophora* transmission alone.

462 Aspects of the framework that can be adapted to represent the host-parasite
463 system of interest are highlighted throughout. For example, parameter *d*, the factor
464 driving arrested development, could be adapted to include immunity (e.g. to simulate
465 the periparturient rise in FECs in ewes), or to extend the estimate of development
466 success (used here for *C. oncophora* and *O. ostertagi*) to include the impacts of
467 desiccation to simulate seasonal arrest in arid regions. In addition, reduced weight
468 gain and parasite-induced anorexia are economically important impacts of GI

nematode infection that have been the focus of many previous models (e.g. Laurenson et al., 2011; Berk et al., 2016a) but were not considered here.

Reduced weight gain could be included in the model by substituting the Cue et al. (2012) equation used here with one that estimates weight gain based on worm burden, and estimating DMI as a function of worm burden to simulate parasite-induced anorexia (e.g. Berk et al., 2016a). The simulations presented here also assumed constant herbage biomass throughout the grazing season due to the lack of data and models to track grass growth. Incorporating models of grass growth, and thus seasonal changes in biomass, may improve predictions by acting on the L3 ingestion rate (i.e. rate of infection, which is a function of DMI rates, total L3 on herbage and available standing biomass). Berk et al. (2016b) incorporated mean monthly grass growth rates for England in their model of *O. ostertagi* in calves. However this, and infection-dependent host growth, was beyond the scope of the current study, which was to develop a minimal, location-independent framework that could be easily parameterised for multiple species and host systems.

GLOWORM-PARA is a mean-field model, simulating the mean trajectory of parasite population dynamics and host immunity in a group of hosts. Mean-field models are useful to explore changes in the system under disparate conditions such as current climate and predicted climate change (Rose et al., 2016), and to evaluate the impact of competing management strategies at a herd/flock level (Learmount et al., 2012). However, in an attempt to stem the development of AR, the focus of parasite control has turned from whole-group treatments to targeted selective treatment (TST), where individuals in a flock/herd are treated either based on parasitological indicators (e.g. FECs in horses and sheep; Kenyon and Jackson, 2012;

493 Matthews and Lester, 2015) or based on performance indicators (e.g. liveweight gain
494 in sheep and cattle; Kenyon and Jackson, 2012). The framework can be adapted to
495 incorporate environmental stochasticity, as demonstrated here, to simulate the
496 heterogeneity of intensity of infection between hosts that forms the basis of
497 selection for TST. This was demonstrated by incorporating stochastic L3 intake rate
498 and immune response in the present study.

499 Limitations of previously published detailed mechanistic approaches include an
500 incomplete understanding of the processes and pathways involved in host immunity
501 to GI nematode infection (although this is disputed by some; Roberts, 1999) and the
502 detailed and invasive immunological datasets required to parameterise these
503 models. The latter is a severe impediment to applying these models to understudied
504 systems and necessitates a more simplified approach to modelling acquired
505 immunity, regardless of whether or not there is an adequate understanding of the
506 underlying processes. Complete representation of relevant immunological pathways,
507 supported by sufficient empirical data to estimate parameters, is therefore difficult
508 to achieve for most GI nematode species and is acknowledged as a bottleneck in the
509 production of mathematical models for the population dynamics of GI nematodes
510 (Charlier et al., 2018).

511 Previous models of GI nematode population dynamics and transmission have
512 differed in their approaches to modelling acquired immunity, which increases during
513 the course of an infection (Claerebout and Vercruysse, 2000). For example, some
514 model acquired immunity as a simple increasing function of the time of exposure to
515 infection (Learmount et al., 2006; Berk et al., 2016a), exposure to larvae (Grenfell et
516 al., 1995), host age (Garnier et al., 2016), or worm burden (Cornell et al., 2004), or

517 mechanistically via the impact of exposure to infection on immunological
518 parameters (Singleton et al., 2011; Prada Jiménez de Cisneros et al., 2014). Practical
519 limitations of the former examples include the absence of upper boundaries on the
520 levels of acquired immunity, which subsequently introduces difficulties scaling
521 immune-mediated parasite life-history parameters. Practical limitations of the latter
522 examples involve the need for invasive immunological measurements (plasma IgA)
523 to estimate immune response rates.

524 The model presented here represents immunity as a logistic growth function. This
525 allows an exponential response with cumulative exposure to GI nematodes,
526 mimicking the stronger immune response that would be expected after
527 administration of a challenge infection or a booster vaccination, and limits acquired
528 immunity to values less than 1 to facilitate modelling interactions between host
529 immune response and parasite life-history parameters. This simple approach also
530 facilitates model application in data-sparse systems. To effectively model the
531 development of host acquired immunity to GI nematodes without explicit
532 representation of the complexities of the immune response and the necessary data
533 for parameterisation, the decay and response rates for the logistic function are
534 estimated using a combination of empirical, non-invasive field data, qualitative
535 observational data and expert judgement. This approach requires fewer data for
536 parameterisation than a more detailed mechanistic representation of immunity, and
537 therefore permits application of this framework to a wider range of host-parasite
538 systems than would be possible with a more detailed model. Nevertheless, there is
539 scope to adapt the representation of immunity as more data become available. It
540 would also be possible, with slight adaptation of the model, to apply varying levels of

host immunity to the different within-host life cycle stages, for example to simulate the use of vaccines with parasite stage-specific activity.

Overall, the mean-field model captured a high proportion of the variability in the observed FECs (*O. ostertagi* mean R^2 = 0.76 and *C. oncophora* mean R^2 = 0.67). Residual error can be attributed to multiple sources, including measurement error in the pasture larval counts used to initiate the model simulations (Couvillion, 1993), multiple sources of variability in the FEC method used in the validation dataset (Levecke et al., 2015), and individual host variability as described above. There was no evidence of systematic bias for *O. ostertagi*, and although the *C. oncophora* model tended to underestimate FECs, the differences in observed and predicted FECs were of no practical significance (section 2.4.4; COWS, 2014). The statistical significance of small deviations in predicted FECs from observed FECs (<25 eggs per gram in herds 1, 2, and 4; Fig. 3) highlights the importance of pragmatic validation methods including statistical, negative binomial models and qualitative appraisal. This is again highlighted by herd 7 which performed poorly in the statistical validation, despite low residual error and high R^2 values (Table 3), and the predicted FECs being within a reasonable range of the observed FECs for both species tested. This was likely due to failure of the model to capture a slight, practically insignificant, increase in FEC for both species mid-August. Despite the overall good performance of the model, there were some exceptions. Herd 1 produced a high *C. oncophora* FEC 1 month after turnout which was not predicted by the model and could be of practical significance, as FECs of the level observed would usually require treatment. The FECs observed for herd 2 were significantly higher than predicted for both species, with differences at the end of the grazing season in the order of several

565 hundred epg. One plausible hypothesis for this, given the good performance of the
566 model for most other herds, is that the individuals on this farm were particularly
567 susceptible to GI nematode infection, which could be due to a number of factors
568 such as genetics, nutrition and coinfection (which cannot be interrogated within the
569 current dataset). Alternatively, the underprediction of FECs on this farm may
570 indicate model bias when applied to young cattle – the calves simulated in Herd 2
571 were the youngest of all the farms used for model validation (6 months, cf. 10-21
572 months). Further validation would be required before applying the model to
573 simulate very young calves (<10 months of age), to determine if this discrepancy is
574 due to the susceptibility of the calves on this farm (posited above), an overestimate
575 of immune response in younger calves, or a non-linear relationship between
576 acquired immunity and the parasitological parameters.

577 To conclude, a generic framework to simulate the parasitic phase of GI nematode
578 infections is presented here and its flexibility is demonstrated by simulating *O.*
579 *ostertagi* and *C. oncophora* infections. The model simulations replicated infection
580 patterns of first season grazers for these nematode species. The lead authors have
581 previously developed a complementary framework for the free-living stages of the
582 GI nematode life cycle, which has been applied to several GI nematode species, and
583 has also been successfully adapted to simulate the development and dispersal of
584 cattle lungworm (*Dictyocaulus viviparus;* McCarthy, C.A., 2018. Predicting the
585 unpredictable: the changing epidemiology of *Dictyocaulus viviparus* in Great Britain.
586 PhD Thesis. University of Liverpool, UK). It is hoped that GLOWORM-PARA will drive
587 similar innovation and international collaboration by providing an accessible and
588 transparent framework that can be adapted to multiple species and extended where

additional detail is required. Future research will integrate GLOWORM-PARA with GLOWORM-FL and host-parasite interactions (host movements, anthelmintic treatments etc.) to obtain a full lifecycle framework for the evaluation of alternative GI nematode control strategies.

Acknowledgements

We acknowledge the E-OBS dataset from the EU-FP6 project ENSEMBLES (http://ensembles-eu.metoffice.com) and the data providers in the ECA&D project (*http://www.ecad.eu*). Model development was funded by the Biotechnology and Biological Sciences Research Council (BBSRC), UK) LoLa Consortium, "BUG: Building Upon the Genome" (Project reference: BB/M003949/1) and the FP7 GLOWORM project (Grant agreement N° 288975CP-TP-KBBE.2011.1.3-04). ERM was also supported by BBSRC project "Integrating ecology and animal science to manage anthelmintic resistance in cattle under climate change" (Project reference: BB/R010250/1)". This article is based upon work from COST Action COMBAR CA16230, supported by European Cooperation in Science and Technology (COST). The authors would also like to thank the collaborating farmers. Pierre Dorny (Institute of Tropical Medicine, Antwerp, Belgium) is acknowledged for providing an expert opinion on decay of immunity in GI nematode infections.

610 **References**

611 Armour, J., 1989. The influence of host immunity on the epidemiology of
612 trichostrongyle infections in cattle. Vet. Parasitol. 32, 5–19.
613 Barger, I. A., Le Jambre, L. F., Georgi, J. R. and Davies, H. I., 1985. Regulation of
614 *Haemonchus contortus* populations in sheep exposed to continuous infection.
615 Int. J. Parasitol., 15, 529-533
616 Berk, Z., Bishop, S.C., Forbes, A.B., Kyriazakis, I., 2016a. A simulation model to
617 investigate interactions between first season grazing calves and Ostertagia
618 ostertagi. Vet. Parasitol. 226, 198-209.
619 Berk, Z., Laurenson, Y.C.S.M., Forbes, A.B., Kyriazakis, I., 2016b. A stochastic model
620 to investigate the effects of control strategies on calves exposed to
621 Ostertagia ostertagi. Parasitol. 143, 1755-1772.
622 Besier, R.B., Kahn, L.P., Sargison, N.D., Van Wyk, J.A., 2016. The pathophysiology,
623 ecology and epidemiology of *Haemonchus contortus* infection in small
624 ruminants. Adv. Parasitol. 93, 95-143.
625 Borgsteede, F.H.M., Hendriks, J., 1973. A quantitative method of cultivating and
626 collecting infective larvae of gastrointestinal nematodes. Tijdschr.
627 Diergeneesk., 98, 280–286
628 Carlsson, A.M., Irvine, R.J., Wilson, K., Coulson, S.J., 2013. Adaptations to the Arctic:
629 low-temperature development and cold tolerance in the free-living stages of
630 a parasitic nematode from Svalbard. Polar Biol. 36, 997-1005.
631 Charlier, J., Demeler, J., Höglund, J., von Samson-Himmelstjerna, G., Dorny, P.,
632 Vercruysse, J., 2010. *Ostertagia ostertagi* in first-season grazing cattle in

633 Belgium, Germany and Sweden: General levels of infection and related
634 management practices. Vet. Parasitol. 171, 91-98.
635 Charlier, J., Höglund, J., von Samson-Himmelstjerna, G., Dorny, P., Vercruysse, J.,
636 2009. Gastrointestinal nematode infections in adult dairy cattle: impact on
637 production, diagnosis and control. Vet. Parasitol. 164, 70-79.
638 Charlier, J., Morgan, E.R., Rinaldi, L., van Dijk, J., Demeler, J., Höglund, J., Hertzberg,
639 H., Van Ranst, B., Hendrickx, G., Vercruysse, J., Kenyon, F., 2014. Practices to
640 optimise gastrointestinal nematode control on sheep, goat and cattle farms
641 in Europe using targeted (selective) treatments. Vet. Rec. 175, 250-255.
642 Charlier, J., Thamsborg, S.M., Bartley, D.J., Skuce, P.J., Kenyon, F., Geurden, T., Hoste,
643 H., Williams, A.R., Sotiraki, S., Höglund, J., Chartier, C., Geldhof, P., van Dijk, J.,
644 Rinaldi, L., Morgan, E.R., von Samson-Himmelstjerna, G., Vercruysse, J.,
645 Claerebout, E., 2018. Mind the gaps in research on the control of
646 gastrointestinal nematodes of farmed ruminants and pigs. Transbound.
647 Emerg. Dis. 65, 217-234.
648 Claerebout, E., Dorny, P., Vercruysse, J., Agneessens, J., Demeulenaere, D., 1998.
649 Effects of preventive anthelmintic treatment on acquired resistance to
650 gastrointestinal nematodes in naturally infected cattle. Vet. Parasitol. 76,
651 287-303.
652 Claerebout, E., Vercruysse, J., 2000. The immune response and the evaluation of
653 acquired immunity against gastrointestinal nematodes in cattle: a review.
654 Parasitol. 120, S25-S42.

655 Cornell, S.J., Isham, V.S., Grenfell, B.T., 2004. Stochastic and spatial dynamics of
656 nematode parasites in farmed ruminants. Proc. R. Soc. Lond. B. Biol. Sci. 271,
657 1243-1250.
658 Couvillion, C.E., 1993. Estimation of the numbers of trichostrongylid larvae on
659 pastures. Vet. Parasitol., 46, 197-203.
660 COWS, 2014. COWS (Control of Worms Sustainably) Technical Manual: Integrated
661 parasite control on cattle farms. Available at:
662 https://www.cattleparasites.org.uk/app/uploads/2018/04/Integrated-
663 parasite-control-on-cattle-farms.pdf Accessed 28th February 2019.
664 Coyne, M. J. and Smith, G., 1992. The mortality and fecundity of *Haemonchus*
665 *contortus* in parasite-naïve and parasite-exposed sheep following single
666 experimental infections. Int. J. Parasitol, 22, 315-325.
667 Cue, R.I., Pietersma, D., Lefebvre, D., Lacroix, R., Wade, K., Pellerin, D., de Passille,
668 A.M., Rushen, J., 2012. Growth modeling of dairy heifers in Quebec based on
669 random regression. Can. J. Anim. Sci. 92, 33-47.
670 Egwang, T. G., Slocombe, J. O. D., 1981. Efficiency and sensitivity of techniques for
671 recovering nematode eggs from bovine faeces. Can. J. Comp. Med. 45, 243-
672 248.
673 Eysker, M., 1993. The Role of Inhibited Development in the Epidemiology of
674 *Ostertagia* Infections. Vet. Parasitol. 46, 259-269.
675 Fernández, A.S., Fiel, C.A., Steffan, P.E., 1999. Study on the inductive factors of
676 hypobiosis of *Ostertagia ostertagi* in cattle. Vet. Parasitol. 81, 295-307.

677 Fox, N.J., Smith, L.A., Houdijk, J.G.M., Athanasiadou, S., Hutchings, M.R., 2018.
678 Ubiquitous parasites drive a 33% increase in methane yield from livestock. Int.
679 J. Parasitol. 48, 1017-1021.

680 Frank, G.R., Herd, R.P., Marbury, K.S., Williams, J.C., 1986. Effects of transfer of
681 *Ostertagia ostertagi* between Northern and Southern USA on the pattern and
682 frequency of hypobiosis. Int. J. Parasitol. 16, 391-398.

683 Garnier, R., Grenfell, B. T., Nisbet, A. J., Matthews, J. B., Graham, A. L., 2016.
684 Integrating immune mechanisms to model nematode worm burden: an
685 example in sheep. Parasitol. 143, 894-904.

686 Grenfell, B. T., Smith, G. and Anderson, R. M., 1987. A mathematical model of the
687 population biology of *Ostertagia ostertagi* in calves and yearlings. Parasitol.
688 95, 389-406

689 Grenfell, B. T., Wilson, K., Isham, V. S., Boyd, H. E. G. and Dietz, K., 1995. Modelling
690 patterns of parasite aggregation in natural populations: trichostrongylid
691 nematode-ruminant interactions as a case study. Parasitol. 111, S135–S151.

692 Haylock, M.R., Hofstra, N., Klein Tank, A. M. G., Klok, E. J., Jones, P. D., New, M., 2008.
693 A European daily high-resolution gridded dataset of surface temperature and
694 precipitation. J. Geophys. Res. (Atmospheres) 113, D20119.

695 Hyndman R. J., Khandakar, Y. 2008. Automatic time series forecasting: the forecast
696 package for R. J. Stat. Software, 26, 1-22.

697 Kahn, L.O., Johsnon, I.R., Rowe, J.B., Hogan, L., Boshoff, J., 2017. ASKBILL as a web-
698 based program to enhance sheep well-being and productivity. Anim. Prod.
699 Sci. 57, 2257-2262.
700 Kenyon, F., Jackson, F., 2012. Targeted flock/herd and individual ruminant treatment
701 approaches. Vet. Parasitol. 186, 10-17.
702 Langrova, I., Jankovska, I., 2004. Arrested development of *Trichostrongylus*
703 *colubriformis* in experimentally infected rabbits. Effect of decreasing
704 photoperiod, low temperature and desiccation. Helminthologia 41, 85-90.
705 Langrova, I., Makovcova, K., Vadlejch, J., Jankovska, I., Petrtyl, M., Fechtner, J., Keil,
706 P., Lytvynets, A., Borkovcova, M., 2008. Arrested development of sheep
707 strongyles: onset and resumption under field conditions of Central Europe.
708 Parasitol. Res. 103, 387-392.
709 Laurenson, Y.C.S.M., Bishop, S.C., Kyriazakis, I., 2011. In silico exploration of the
710 mechanisms that underlie parasite-induced anorexia in sheep. British J.
711 Nutrition 106, 1023-1039.
712 Learmount, J., Callaby, R., Taylor, M., 2018. An observational study of ewe
713 treatments at lambing on early infection in lambs on UK sheep farms. Vet.
714 Parasitol. 253, 55-59.
715 Learmount, J., Taylor, M.A., Bartram, D.J., 2012. A computer simulation study to
716 evaluate resistance development with a derquantel-abamectin combination
717 on UK sheep farms. Vet. Parasitol. 187, 244-253.
718 Learmount, J., Taylor, M.A., Smith, G., Morgan, C., 2006. A computer model to
719 simulate control of parasitic gastroenteritis in sheep on UK farms. Vet.
720 Parasitol. 142, 312-329.

721 Leathwick, D.M., Barlow, N.D., Vlassoff, A., 1992. A model for nematodiasis in New-
722 Zealand lambs. Int. J. Parasitol. 22, 789-799.
723 Leathwick, D.M., Donecker, J.M., Nielsen, M.K., 2015. A model for the dynamics of
724 the free-living stages of equine cyathostomins. Vet. Parasitol. 209, 210-220.
725 Leathwick, D.M., Sauermann, C.W., Donecker, J.M., Nielsen, M.K., 2016. A model for
726 the development and growth of the parasitic stages of *Parascaris* spp. In the
727 horse. Vet. Parasitol. 228, 108-115.
728 Leathwick, D.M., Sauermann, C.W., Geurden, T., Nielsen, M.K., 2017. Managing
729 anthelmintic resistance in *Parascaris* spp.: A modelling exercise. Vet. Parasitol.
730 240, 75-81.
731 Levecke, B., Rinaldi, L., Charlier, J., Maurelli, M.P., Morgoglione, M.E., Vercruysse, J.,
732 Cringoli G., 2011. Monitoring drug efficacy against gastrointestinal
733 nematodes when faecal egg counts are low: do the analytic sensitivity and
734 the formula matter? Parasitol. Res., 109, 953–957.
735 Levecke. B., Anderson, R.M., Berkvens, D., Charlier, J., Devleesschauwer, B.,
736 Speybroeck. N., Vercruysse, J., Van Aelst, S., 2015. Mathematical Inference on
737 Helminth Egg Counts in Stool and Its Applications in Mass Drug
738 Administration Programmes to Control Soil-Transmitted Helminthiasis in
739 Public Health. Adv. Parasitol., 87, 193-247.
740 Lützelschwab, C.M., Fiel, C.A., Pedonesse, S.I., Najle, R., Rodriguez, E., Steffan, P.E.,
741 Saumell, C., Fuse, L., Iglesias, L., 2005. Arrested development of *Ostertagia*
742 *ostertagi*: effect of the exposure of infective larvae to natural spring
743 conditions of the Humid Pampa (Argentina). Vet. Parasitol. 127, 253-262.

744 MAFF (Ministry of Agriculture, Fisheries and Food), 1975. Energy allowances and
745 feeding systems for ruminants. Tech. Bull., 33 Ministry of Agriculture and
746 Fisheries. Her Majesty's Stationery Office, London.
747 MAFF, 1986. Technical Bulletin No. 18, Manual of veterinary parasitological
748 laboratory techniques. London: Her Majesty's Stationery Office, London, UK.
749 Matthews, J.B., Geldhof, P., Tzelos, T., Claerebout, E., 2016. Progress in the
750 development of subunit vaccines for gastrointestinal nematodes of
751 ruminants. Parasite Immunol. 38, 744-753.
752 Matthews, J., Lester, H., 2015. Control of equine nematodes: making the most of
753 faecal egg counts In Practice 37, 540 - 544.
754 Mavrot, F., Hertzberg, H., Torgerson, P., 2015. Effect of gastro-intestinal nematode
755 infection on sheep performance: a systematic review and meta-
756 analysis. Parasites Vectors, 8, 557.
757 Michel, J.F., Lancaster, M.B., Hong, C., 1976. Observations on resumed development
758 of arrested *Ostertagia ostertagi* in naturally infected yearling cattle. J. Comp.
759 Pathol. 86, 73-80.
760 Molnár, P.K., Kutz, S.J., Hoar, B.M., Dobson, A.P., 2013. Metabolic approaches to
761 understanding climate change impacts on seasonal host-macroparasite
762 dynamics. Ecol. Lett. 16, 9-21.
763 Morgan, E.R., Aziz, N-A., Blanchard, A., Charlier, J., Charvet, C., Claerebout, E.,
764 Geldhof, P., Greer, A.W., Hertzberg, H., Hodgkinson, J., Höglund, J., Hosta, H.,
765 Kaplan, R.M., Martinez-Valladares, M., Mitchell, S., Ploeger, H.W., Rinaldi, L.,
766 von Samson-HImmelstjerna, G., Sotiraki, S., Schnyder, M., Skuce, P., Bartley,
767 D., Kenyon, F., Thamsborg, S.M., Rose Vineer, H., de Waal, T., Williams, A.R.,

768 Van Wyk, J.A., Vercruysse, J., 2018. 100 questions in livestock helminthology
769 research. Trends Parasitol. 35, 52-71.
770 Morgan, E.R., 2013. Detail and the devil of on-farm parasite control under climate
771 change. Anim. Health. Res. Rev. 14, 138-142.
772 Morgan, E.R., van Dijk, J., 2012. Climate and the epidemiology of gastrointestinal
773 nematode infections of sheep in Europe. Vet. Parasitol. 189, 8-14.
774 Moritz, S., Bartz-Beielstein, T., 2017. imputeTS: time series missing value imputation
775 in R. R Journal 9, 27-218.
776 Nennich, T.D., Harrison, J.H., VanWieringen, L.M., Meyer, D., Heinrichs, A.J., Weiss,
777 W.P., St-Pierre, N.R., Kincaid, R.L., Davidson, D.L., Block, E., 2005. Prediction
778 of manure and nutrient excretion from dairy cattle. J. Dairy Sci. 88, 3721-
779 3733.
780 Nieuwhof, G.J., Bishop, S.C., 2005. Costs of the major endemic diseases of sheep in
781 Great Britain and the potential benefits of reduction in disease impact. Anim.
782 Sci. 81, 23-29.
783 Paras, K.L., George, M.M., Vidyashankar, A.N., Kaplan, R.M., 2018. Comparison of
784 fecal egg counting methods in four livestock species. Vet. Parasitol. 257, 21-
785 27.
786 Ploeger, H.W., Kloosterman, A., Rietveld, F.W., 1995. Acquired immunity against
787 *Cooperia* spp. and *Ostertagia* spp. in calves - Effect of level of exposure and
788 timing of the midsummer increase. Vet. Parasitol. 58, 61-74.
789 Powers, K.G., Wood, I.B., Eckert, J., Gibson, T., Smith, H.J., 1982. World Association
790 for the Advancement of Veterinary Parasitology (W.A.A.V.P.) guidelines for

791 evaluating the efficacy of anthelmintics in ruminants (bovine and ovine). Vet.
792 Parasitol. 10, 265-284.
793 Prada Jiménez de Cisneros, J., Stear, M. J., Mair, C., Singleton, D., Stefan, T., Stear, A.,
794 Marion, G., Matthews, L., 2014. An explicit immunogenetic model of
795 gastrointestinal nematode infection in sheep. J. R. Soc. Interface 11,
796 20140416.
797 Ravinet, N., Bareille, N., Lehebel, A., Ponnau, A., Chartier, C., Chauvin, A., 2014.
798 Change in milk production after treatment against gastrointestinal
799 nematodes according to grazing history, parasitological and production-
800 based indicators in adult dairy cows. Vet. Parasitol. 201, 95-109.
801 Rendle, D., Austin, C., Bowen, M., Cameron, I., Furtado, T., Hodgkinson, J., McGorum,
802 B., Matthews, J., 2019. Equine de-worming: a consensus on current best
803 practice. UK-Vet Equine, 3, 1.
804 Roberts, M.G., Grenfell, B.T., 1991. The population-dynamics of nematode infections
805 of ruminants - Periodic perturbations as a model for management. Ima. J.
806 Math. Appl. Med. 8, 83-93.
807 Roberts, M.G., 1999. The Immunoepidemiology of Nematode Parasites of Farmed
808 Animals: A Mathematical Approach. Trends Parasitol., 15, 246-251.
809 Rose, H., Caminade, C., Bolajoko, M. B., Phelan, P., van Dijk, J., Baylis, M., Williams,
810 D., Morgan, E. R., 2016. Climate-driven changes to the spatio-temporal
811 distribution of the parasitic nematode, *Haemonchus contortus*, in sheep in
812 Europe. Glob. Change Biol. 22, 1271–1285.

Rose, H., Hoar, B., Kutz, S.J., Morgan, E.R., 2014. Exploiting parallels between livestock and wildlife: predicting the impact of climate change on gastrointestinal nematodes in ruminants. Int. J. Parasitol. Parasites Wildlife. 2, 209-219.

Rose, H., Wang, T., Van Dijk, J., Morgan, E.R., 2015. GLOWORM-FL: A simulation model of the effects of climate and climate change on the free-living stages of gastro-intestinal nematode parasites of ruminants. Ecol. Model. 297, 232-245.

Salisbury, E., Thistlethwaite, G., Goodwin, J., MacCarthy, J., 2015. Emissions of the basket of 7 Kyoto GHGs according to Devolved Administration 1990-2013.: Accessed 20/01/19 at: http://naei.defra.gov.uk/reports/reports?report_id=810

Sauermann, C.W., Leathwick, D.M., 2018. A climate-driven model for the dynamics of the free-living stages for *Cooperia oncophora*. Vet. Parasitol. 255, 83-90.

Shaw, D.J., Vercruysse, J., Claerebout, E., Agneessens, J., Dorny, P., 1997. Gastrointestinal nematode infections of first-season grazing calves in Belgium: general patterns and the effect of chemoprophylaxis. Vet. Parasitol. 69, 103-116.

Shaw, D.J., Vercruysse, J., Claerebout, E., Dorny, P., 1998. Gastrointestinal nematode infections of first-grazing season calves in western Europe: general patterns and the effect of chemoprophylaxis. Vet. Parasitol. 75, 115-131.

Singleton, D. R., Stear, M. J., Matthews, L., 2011. A mechanistic model of developing immunity to *Teladorsagia circumcincta* infection in lambs. Parasitol. 138, 322-332.

837 Skuce, P.J., Morgan, E.R., van Dijk, J., Mitchell, M., 2013. Animal health aspects of
838 adaptation to climate change: beating the heat and parasites in a warming
839 Europe. Animal 7, 333-345.
840 Smith, G., 1994. Population biology of the parasitic phase of trichostrongylid
841 nematode parasites of cattle and sheep. Int. J. Parasitol. 24, 167-178
842 Smith, G., 2011. Models of macroparasitic infections in domestic ruminants: a
843 conceptual review and critique. Rev. Sci. Tech. Oie. 30, 447-456.
844 Smith, G. and Grenfell, B. T., 1985. The population biology of *Ostertagia ostertagi*.
845 Parasitol. Today, 1, 76-81
846 Smith, H.J., 1974. Inhibited development of *Ostertagia ostertagi*, *Cooperia*
847 *oncophora* and *Nematodirus helvetianus* in parasite-free calves grazing fall
848 pastures. Am. J. Vet. Res. 35, 935-938.
849 Smith, W. D., Jackson, F., Jackson, E. and Williams, J., 1985. Age immunity to
850 *Ostertagia circumcincta*: Comparison of the local immune responses of 4 1/2-
851 and 10-month-old lambs. J. Comparative Path. 95, 235-245.
852 Soetaert, K., Petzoldt, T., Setzer, R.W. 2010. Solving Differential Equations in R:
853 Package deSolve. J. Stat. Software, 33, 1-25.
854 Stear, M. J., Bishop, S. C., Doligalska, M., Duncan, J. L., Holmes, P. H., Irvine, J.,
855 McCririe, L., McKellar, Q. A., Sinski, E. and Murray, M., 1995. Regulation of
856 egg production, worm burden, worm length and worm fecundity by host
857 responses in sheep infected with *Ostertagia circumcincta*. Parasite Immunol,
858 17, 643-652

859 Stear, M. J., Fitton, L., Innocent, G. T., Murphy, L., Rennie, K. and Matthews, L., 2007.
860 The dynamic influence of genetic variation on susceptibility of sheep to
861 gastrointestinal nematode infection. J. Royal. Soc. Interface. 4, 767-776.
862 Sutherland, I.A., Leathwick, D.M., 2011. Anthelmintic resistance in nematode
863 parasites of cattle: a global issue? Trends Parasitol. 27, 176-181.
864 Taylor, E.L., 1939. Technique for the estimation of pasture infestation by strongyloid
865 larvae. Parasitol. 31, 473–478.
866 Verschave, S.H., Charlier, J., Rose, H., Claerebout, E., Morgan, E.R., 2016a. Cattle and
867 nematodes under global change: transmission models as an ally. Trends
868 Parasitol. 32, 724-738.
869 Verschave, S.H., Levecke, B., Duchateau, L., Vercruysse, J., Charlier, J., 2015.
870 Measuring larval nematode contamination on cattle pastures: Comparing
871 two herbage sampling methods. Vet. Parasitol. 210, 159-166.
872 Verschave, S.H., Vercruysse, J., Claerebout, E., Rose, H., Morgan, E. R. and Charlier, J.,
873 2014a. The parasitic phase of *Ostertagia ostertagi*: quantification of the main
874 life history traits through systematic review and meta-analysis. Int. J.
875 Parasitol. 44, 1091-1104.
876 Verschave, S. H., Vercruysse, J., Forbes, A., Opsomer, G., Hostens, M., Duchateau, L.,
877 Charlier, J., 2014b. Non-invasive indicators associated with the milk yield
878 response after anthelmintic treatment at calving in dairy cows. BMC Vet. Res.
879 10, 264.
880 Verschave, S.H., Rose, H., Morgan, E. R., Claerebout, E., Vercruysse, J. and Charlier, J.,
881 2016b. Modelling *Cooperia oncophora*: quantification of key parameters in
882 the parasitic phase. Vet. Parasitol. 223, 111-114

883 Vercruysse, J. and Claerebout, E., 1997. Immunity development against *Ostertagia*
884 *ostertagi* and other gastrointestinal nematodes in cattle. Vet. Parasitol. 72,
885 309-326.

886

887 **Figure legends**

888

889 Fig. 1. Conceptual framework of the GLOWORM-PARA model. State variable and
890 parameter definitions are given in Table 1. Solid arrows indicate life-cycle transitions
891 (e.g. from ingested L3 (L3i) to pre-adult (P) to adult (A)), mortality (μ_i) or deposition
892 of eggs (λ). Dashed arrows indicate dependencies (e.g. the level of acquired
893 immunity (r) depends on the intake of L3 (L3i)).

894

895 Fig. 2. Observed and predicted faecal egg counts (FEC) for *Ostertagia ostertagi* in
896 first season grazing animals of dairy herds in Belgium. FECs were monitored for the
897 entire length of the first grazing season. Further information on the background of
898 this data can be found in Supplementary Table S1. Points and error bars show the
899 observed number of eggs per gram of faeces (epg) and the corresponding 95%
900 confidence interval obtained by bootstrapping (10,000 repeats). The dashed black
901 line depicts the predicted FEC for a group of hosts based on a deterministic model
902 simulation. The solid grey lines depict predictions obtained from 50 model
903 simulations representing individual hosts, in which stochastic L3 intake and
904 between-host variability in immune response were incorporated.

905

906 Fig. 3. Observed and predicted faecal egg counts (FEC) for *Cooperia oncophora* in
907 first season grazing animals of dairy herds in Belgium. FECs were monitored for the
908 entire length of the first grazing season. Further information on the background of
909 this data can be found in Supplementary Table S1. Points and error bars show the
910 observed number of eggs per gram of faeces (epg) and the corresponding 95%

911 confidence interval obtained by bootstrapping (10,000 repeats). The dashed black
912 line depicts the predicted FEC for a group of hosts based on a deterministic model
913 simulation. The solid grey lines depict predictions obtained from 50 model
914 simulations representing individual hosts, in which stochastic L3 intake and
915 between-host variability in immune response were incorporated.
916
917 Fig. 4. The observed and simulated faecal egg counts (FECs; points) with 95%
918 confidence intervals (observed = horizontal, simulated = vertical). The diagonal black
919 line indicates hypothetical perfect agreement between the observed and simulated
920 FECs. The grey solid line indicates the predicted slope of the regression, with 95%
921 confidence intervals show as grey dashed lines. Note that the 95% confidence
922 intervals for the simulated data (estimated using the stochastic simulations shown in
923 grey in Figs. 2 and 3) are narrow and may not be easily seen due to the scale of the
924 Y-axes.
925
926 Supplementary Fig. S1. Mean daily temperature (A) and total daily rainfall (B) for the
927 observation period for each herd used for model validation. Data were obtained from
928 the E-OBS gridded dataset (Haylock et al., 2008) based on the village where each herd
929 was located (Supplementary Table S1).
930 **Reference**
931 Haylock, M.R., Hofstra, N., Klein Tank, A. M. G., Klok, E. J., Jones, P. D., New, M., 2008. A
932 European daily high-resolution gridded dataset of surface temperature and precipitation. J.
933 Geophys. Res. (Atmospheres) 113, D20119.
934
935 **Highlights**
936

- The transmission of gastrointestinal nematode parasitic stages was modelled
- The generic model was parameterised for *Cooperia oncophora* and *Ostertagia ostertagi* in cattle
- Extensive validation using field data demonstrated good model performance
- A pragmatic approach to modelling data-sparse systems (immunity) is demonstrated
- Stochastic parameters can be introduced to incorporate host variability

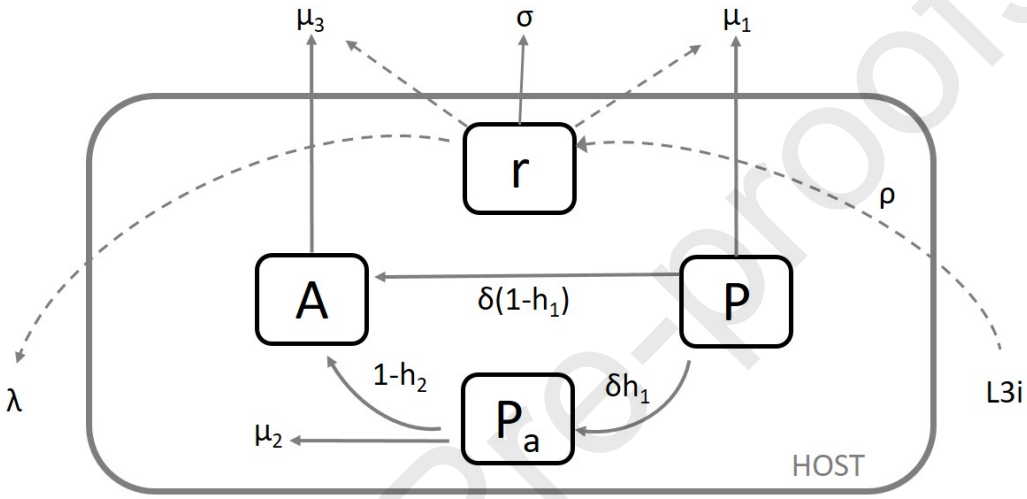

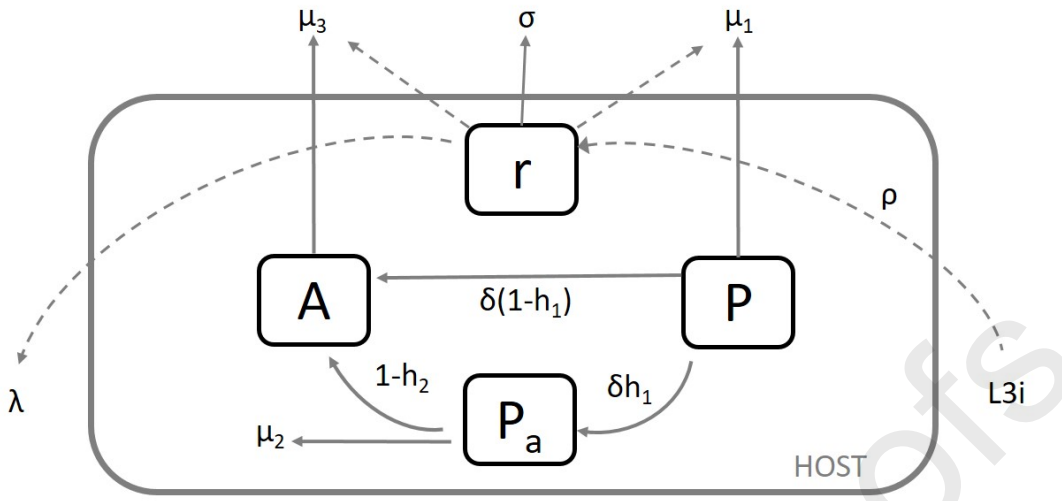

947

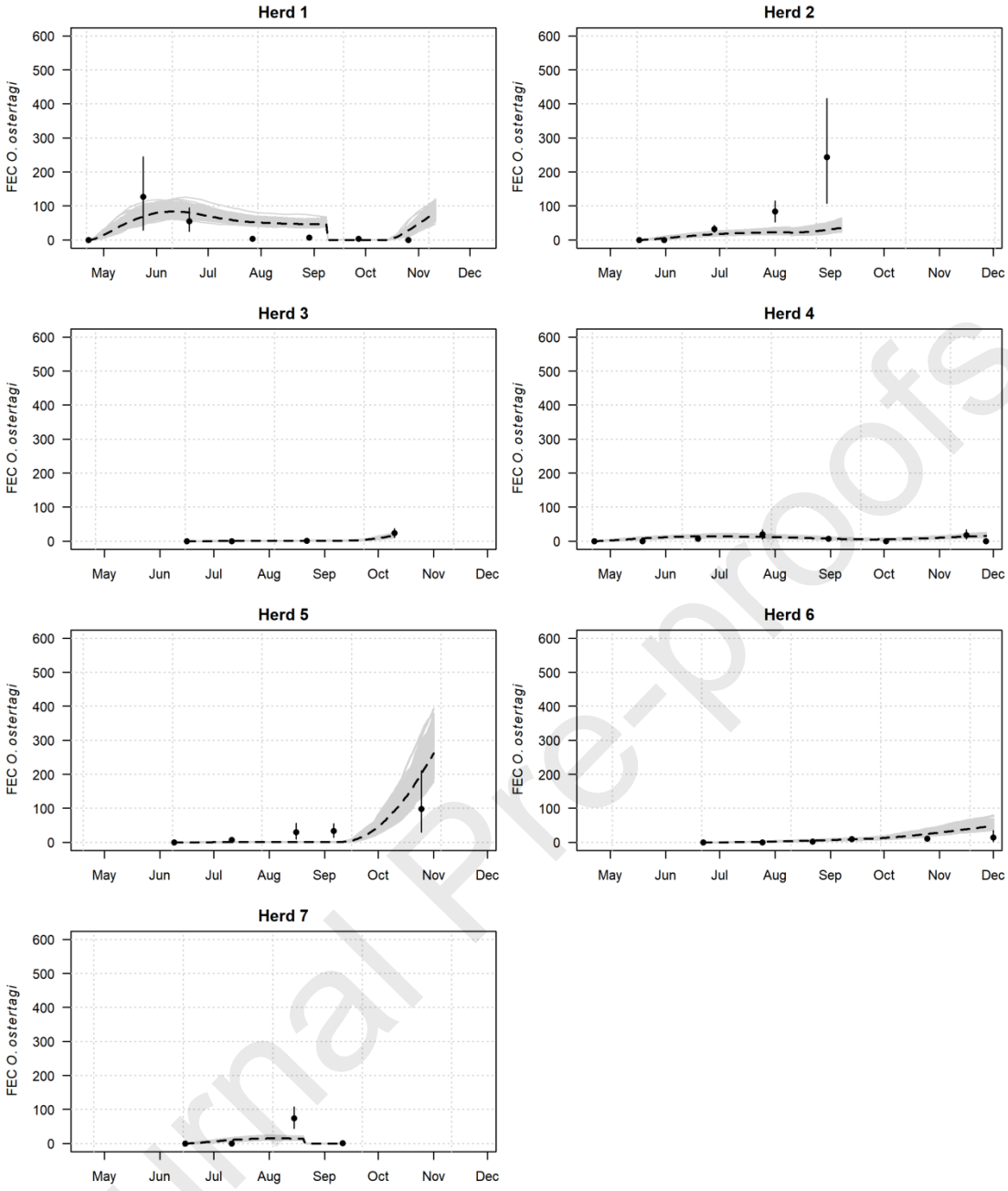

948

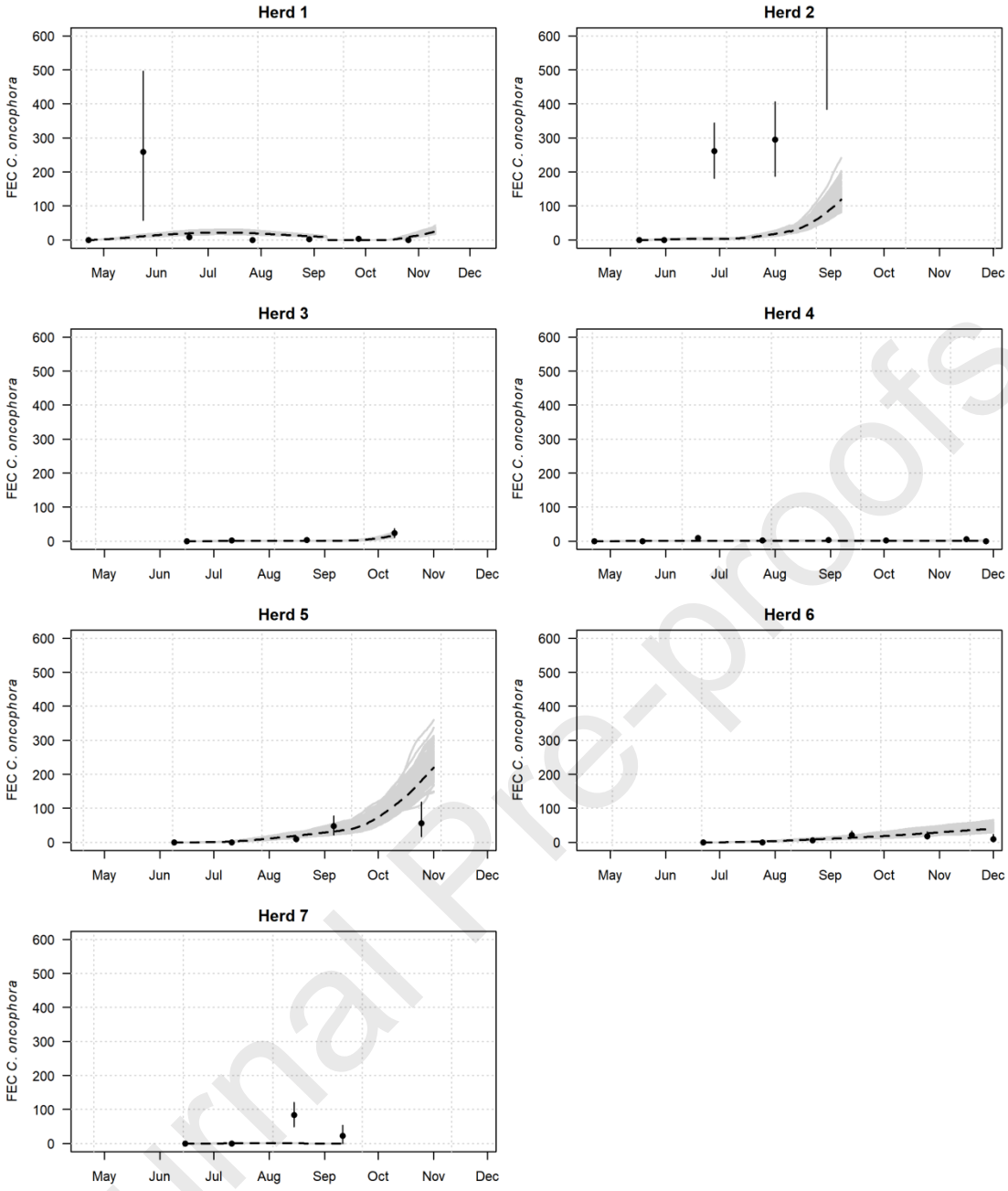

949

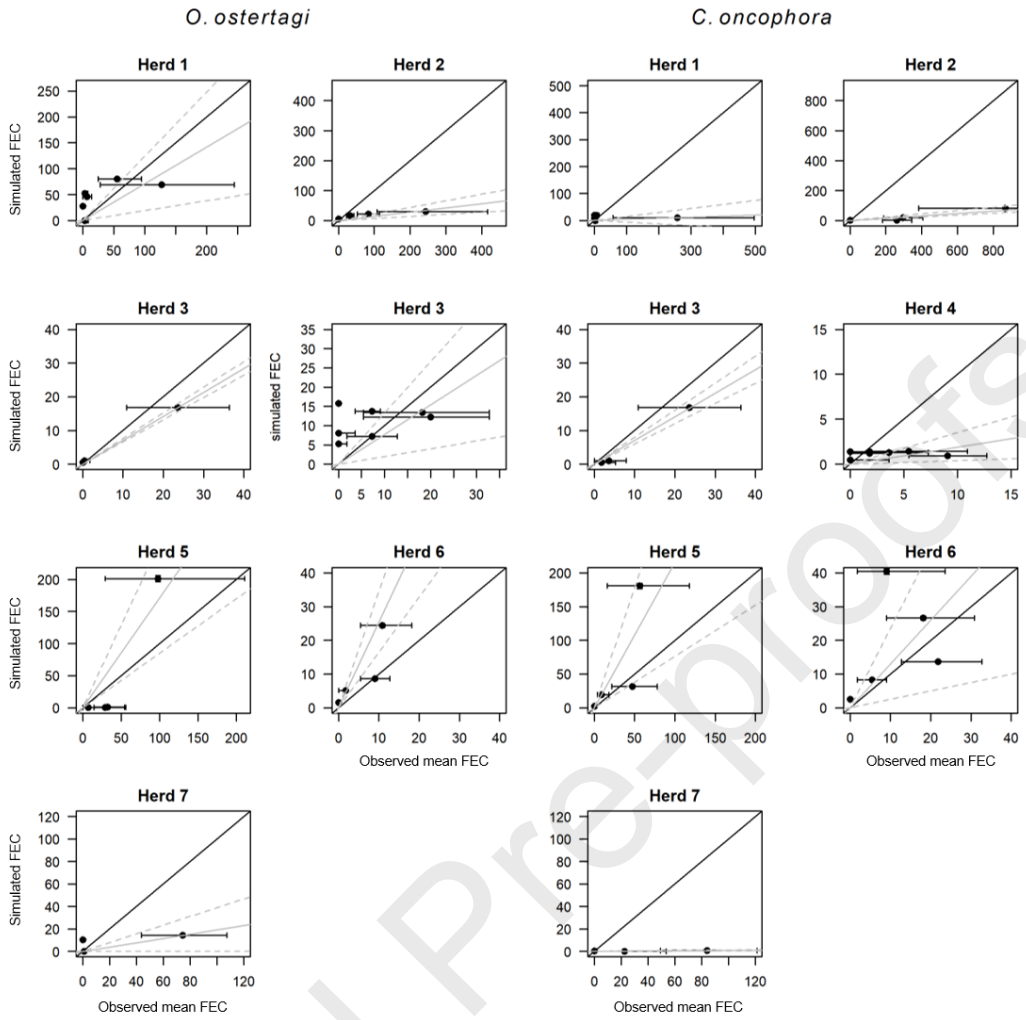

950

951 **Table 1.** Model state variable and parameter definitions

State variable (bold) or Parameter	Definition	Units
P	Pre-adult nematodes in the host (L3, L4 and immature adult)	-
Pa	Arrested L4	-
A	Mature adult	-
r	Acquired immunity	-
L3h	L3 density on herbage	L3 kg dry matter^{-1}
L3i	L3 ingestion rate	L3 day^{-1} host^{-1}
δ	Development rate from ingested L3 to mature adult	P^{-1} day^{-1}
μ_1	Pre-adult mortality rate	P^{-1} day^{-1}

μ_2	Arrested L4 mortality rate	Pa^{-1} day^{-1}
μ_3	Adult mortality rate	A^{-1} day^{-1}
h_1	Rate of developing pre-adult nematodes entering arrested development	P^{-1} day^{-1}
h_2	Rate of arrested larvae resuming development	Pa^{-1} day^{-1}
ρ	Immune response	$L3i^{-1}$
σ	Immune decay	Day^{-1}
λ	Daily fecundity (eggs produced)	Eggs $worm^{-1}$ day^{-1}
f	Daily faeces production	Grams (wet weight) day^{-1}
d	Driver of arrest	N/A[a]
DMI	Daily herbage dry matter intake	Grams day^{-1}
kgDM	Standing biomass (herbage) on pasture	kg dry matter $hectare^{-1}$
FEC	Faecal egg count	Eggs $gram^{-1}$

[a] As this parameter is used to scale the immune-dependent parameters, the unit need not be fixed. In the present study, the temperature-dependent development rate of *Ostertagia ostertagi* or *Cooperia oncophora* has been used as an indicator of development success. However other, more complex, indicators can be used where sufficient data exist for parameterisation, such as Q_0 estimates or the proportion of eggs surviving to L3 on pasture, or this parameter can be adapted to incorporate immunity-driven arrested development.

Table 2. Parameter estimates for *Ostertagia ostertagi* (*Oo*) and *Cooperia oncophora* (*Co*).

Parameter	***Species***	***Estimate***	***Source***
$\boldsymbol{\delta}$	*Oo, Co*	-ln(0.5)/17= 0.041	Powers et al. (1982)
$\boldsymbol{\mu_{1(min)}}$	*Oo*	0.054	Mean in Verschave et al. (2014a)
	Co	0.044	Mean in Verschave et al. (2016b)
$\boldsymbol{\mu_{1(max)}}$	*Oo*	0.062	Upper 95% CI in Verschave et al. (2014a)
	Co	0.052	Upper 95% CI in Verschave et al. (2016b)
$\boldsymbol{\mu_2}$	*Oo, Co*	0.002	Grenfell et al. (1987)
$\boldsymbol{\mu_{3(min)}}$	*Oo*	0.028	Mean in Verschave et al. (2014a)
	Co	0.039	Mean in Verschave et al. (2016b)
$\boldsymbol{\mu_{3(max)}}$	*Oo*	0.032	Upper 95% CI in Verschave et al. (2014a)

	Co	0.048	Upper 95% CI in Verschave et al. (2016b)
$h_{(min)}$	*Oo*	0.02	Lower 95% CI in Verschave et al. (2014a)
	Co	0.004	Lower 95% CI in Verschave et al., (2016b)
$h_{(max)}$	*Oo*	0.06	Upper 95% CI in Verschave et al. (2014a)
	Co	0.011	Upper 95% CI in Verschave et al. (2016b)
ρ	*Oo*	5.981×10^{-5}	Current study (fitted to data from Shaw et al. (1998), see main text for assumptions)
	Co	1.316×10^{-4}	Current study (fitted to data from Shaw et al. (1998), see section 2.3.3. for assumptions)
σ	*Oo, Co*	-ln(0.7)/(6*30) = 0.002	Current study (expert opinion)
$\lambda_{(min)}$	*Oo*	ln(196/2) = 4.58	Lower 95% CI in Verschave et al. (2014a)
	Co	ln(1253/2) = 6.44	Lower 95% CI in Verschave et al. (2016b)
$\lambda_{(max)}$	*Oo*	ln(284/2) = 4.96	Mean in Verschave et al. (2014a), assuming a 1:1 sex ratio
	Co	ln(2968/2) = 7.30	Mean in Verschave et al. (2016b); assuming a 1:1 sex ratio
d	*Oo*	$-0.07258 + 0.00976T^a$	Rose et al. (2015)
	Co	$-0.0401 + 0.00821T^a$	Current study (fitted to data from Sauermann and Leathwick (2018))

962 [a]T = daily mean air temperature (°C)

963 CI, Confidence Interval.

964

965 **Table 3.** Validation of simulations for faecal egg counts (FECs) of *Ostertagia*
966 *ostertagi* and *Cooperia oncophora* using parasitological data of first season
967 grazing animals on seven commercial dairy herds in Belgium.

	Ostertagia ostertagi				*Cooperia oncophora*			
Data set	Error (residual sum of squares)	Linear regression	R^2 (R^2 adjusted)	Slope (95% CI)	Error (residual sum of squares)	Linear regression	R^2 (R^2 adjusted)	Slope (95% CI)
Herd 1	37.69	$F_{1,5}$=6.89, P=0.047	0.58 (0.50)	0.71 (0.19 – 1.24)	13.75	$F_{1,5}$=0.69, P=0.445	0.12 (-0.06)	0.04 (-0.06 – 0.15)
Herd 2	10.11	$F_{1,3}$=13.35, P=0.035	0.82 (0.76)	0.14 (0.07 – 0.22)	12.62	$F_{1,3}$=41.06, P=0.008	0.93 (0.91)	0.08 (0.06 – 0.11)
Herd 3	0.61	$F_{1,2}$=766.7, P=0.001	1 (1)	0.71 (0.66 – 0.76)	1.21	$F_{1,2}$=191.3, P=0.005	0.99 (0.98)	0.70 (0.60 – 0.80)
Herd 4	8.38	$F_{1,6}$=7.00, P=0.038	0.54 (0.46)	0.77 (0.20 – 1.33)	0.92	$F_{1,6}$=5.90, P=0.051	0.50 (0.41)	0.19 (0.04 – 0.35)
Herd 5	47.31	$F_{1,3}$=15.1, P=0.030	0.83 (0.78)	1.71 (0.85 – 2.57)	53.02	$F_{1,3}$=9.12, P=0.057	0.75 (0.67)	2.16 (0.76– 3.56)
Herd 6	9.42	$F_{1,4}$=30.35, P=0.005	0.88 (0.85)	2.54 (1.64 – 3.45)	16.25	$F_{1,4}$=5.9, P=0.07	0.60 (0.50)	1.30 (0.25– 2.35)
Herd 7	7.39	$F_{1,2}$=3.84, P=0.189	0.66 (0.49)	0.19 (-0.0002 – 0.39)	0.24	$F_{1,2}$=6.48, P=0.126	0.76 (0.65)	0.007 (0.002 – 0.013)

968 CI, Confidence Interval.

969